RSNA 2023 Edition

UNITED IMAGING

Issue Highlights

Deep Learning-Based Reconstruction of Coronary CT Angiography in Patients with Diverse Anatomical and Pathological Complexities

Dijia Wu, et al.
Page 08

Clinical Evaluation of Advanced Algorithms for CCTA: A Focus on High BMI and Elevated Heart Rate Populations

John Osborne, et al.
Page 24

A Vision for Magnetic Resonance Imaging to Assess Cardiotoxicity

Mary P. Watkins, et al.
Page 47

Expert Interview: Cardiac Imaging, Inc. Interview with Jens Huettges

Jens Huettges
Page 63

Disclaimer

The articles contained in this magazine are provided solely by the authors, and the author(s) of each article appearing in this magazine is/are solely responsible for the content thereof as well as personal data, which is used anonymously or in compliance with applicable data privacy laws or regulations. United Imaging Healthcare makes no representation or warranties, expressly or impliedly, with respect to the accuracy, timeliness, reliability, legitimacy, applicability, fitness, originality, or completeness of the contents of this magazine. United Imaging Healthcare assumes no legal responsibility or liability for any error, omission, or illegality with respect to the material contained within.

All articles contained in this magazine only represent the opinions and views of the authors and do not implicitly or explicitly represent any official positions or policies, or medical opinions of United Imaging Healthcare or the institutions with which the authors are affiliated unless this is clearly specified. Discussions of any brand, services, or products in the magazine should not be construed as promotion or endorsement thereof.

Articles published in this magazine are intended to inspire further general scientific research, investigation, understanding, and discussion only and are not intended to and should not be relied upon as recommending or promoting a specific medical advice, method, diagnosis, or treatment by physicians for any particular individual, nor to replace the advice of a physician or other healthcare professional. Any individual wishing to apply the information in this magazine for the purposes of improving their own health should not do so without consulting with a qualified medical practitioner. All patients need to be treated in an individual manner by their personal medical advisors. The decision to utilize any information in this magazine is ultimately at the sole discretion of the reader, who assumes full responsibility for any and all consequences arising from such a decision. United Imaging Healthcare makes no representations or warranties with respect to any treatment, action, or application of medication or preparation by any person following the information offered or provided within or through the magazine.

The articles included in this magazine may contain work in progress, which represents ongoing research and development. Such technologies are not available for sale in China or the United States for clinical use and also may not be available for such sales in other countries.

Please note that the magazine is intended to be distributed within a limited scope.

If you have any questions about the magazine, or simply wish to reach out to us for any other reasons, you may contact us at: compliance@united-imaging.com

Role of Cardiac T1, T2 Mapping and Extracellular Volume in the Diagnosis of Clinical Cardiomyopathies

Kamal Aggarwal[a], Dharmesh Singh[b], Anjali Anand[b], Dileep Kumar[b]
[a]Department of Radiology, SSB Faridabad, India
[b]Central Research Institute, Global Scientific Collaborations, United Imaging Healthcare, Shanghai, China

1. Introduction

Cardiomyopathy refers to diseases of the heart muscle that affect the heart's ability to pump blood effectively. There are different types of cardiomyopathies, with dilated cardiomyopathy (DCM) and ischemic cardiomyopathy (ICM) being two major clinical forms [1] [2]. Cardiac magnetic resonance (CMR) imaging is commonly used in a variety of cardiovascular diseases [3]. The primary advantage of CMR is its ability to examine and characterize myocardial tissues. T1 and T2 mapping sequences have been incorporated into standard CMR imaging techniques and are rapidly establishing as gold standard [4].

The conventional sequences are primarily focused on magnetic characteristic, such as T1 relaxation for the purpose of scar imaging, commonly referred to as late gadolinium enhancement (LGE), and T2 relaxation for visualizing edema. T1 relaxation time characterizes each tissue precisely since it depends on the molecular environment of the water molecules in the tissue [5]. Another tissue-specific time measure, T2 relaxation time is utilized to distinguish between normal and abnormal cardiac tissues as well as myocardial edema [6]. However, T2-weighted sequences are particularly susceptible to artifacts. The inability to differentiate global cardiac diseases such as pan-inflammation or prominent fibrosis is a significant shortcoming of these conventional sequences.

Advances approaches such as T1 and T2 mappings were developed and evolved significantly in recent years [4]. A single breath-hold method (mainly performed in short-axis views) is used to generate T1 and T2 maps of the myocardium [7]. These use colored pixel maps to represent T1 or T2 values. In contrast to T2 mapping, T1 mapping can be performed without contrast agent administration, referred to as native T1 mapping. Additionally, T1 mapping can also be performed after the administration of a contrast agent, known as post-contrast T1 mapping. Native T1 values are higher in cardiac diseases such as fibrosis, edema which causing an increase in the extracellular compartment compared to healthy volunteers [8][9]. Renal clearance, gadolinium dose, acquisition time post-bolus injection, hematocrit level, and body composition affect post-contrast T1 mapping values. Extracellular volume fraction (ECV) has been shown to provide a more precise measure of tissue perfusion by subtracting pre- and post-contrast maps with hematocrit correction at adequate equilibrium, which typically occurs 15 minutes after bolus injection [10]. ECV is determined using a formula that integrates hematocrit value, native T1, and post contrast T1. Increased ECV is an indicator of cardiac degeneration that is most caused by excessive collagen deposition (in the absence of amyloid or edema) [10]. T2 mapping identifies myocardial edema in acute infarction and inflammatory disease [11].

Kellman and Hansen [12] reported myocardial ECV in healthy volunteers to be similar at field strengths of 1.5T (0.25) and 3 T (0.26). Giri et al. reported normal myocardial T2 values acquired using steady-state free precession (SSFP) MR imaging [13]. The incremental utility of image-based cardiovascular diagnosis using ML for various types of significant diseases, such as coronary artery disease (CAD) and heart failure, has already been demonstrated in previous studies [14],[15].

In summary, native T1, ECV and T2 values have proved to be promising parameters in the field of cardiac imaging. Machine learning based analysis has not been thoroughly evaluated for the diagnostic classification of active cardiomyopathy conditions using T1, ECV and T2 together. The objective of this study was to examine the additional efficacy of T1 mapping, T2 mapping, and ECV in the diagnosis of cardiomyopathies in a clinical setting.

2. Materials and Methods

2.1 MRI data

This prospective study used an MRI dataset of 32 subjects (age: 45 ± 15 years) who had abnormal left ventricle (LV) ejection fraction and were suspected of having cardiac diseases, specifically DCM and ICM with approval from the Institutional Review Board. Scanning was performed on a 1.5T MR scanner (uMR 580, United Imaging Healthcare Co., Ltd., Shanghai, China) at SSB Hospital, Faridabad using a dedicated cardiac coil from January 2023 to May 2023. The CMR protocol comprised gated fast spin echo (FSE) T1, FSE T2, and cine in axial, long axis, and short axis planes with SSFP sequences aligned to 2 chamber view, 4 chamber views well as T1 and T2 mapping. Intravenous gadolinium-based contrast agent with a dose of 0.15 mmol/kg was injected, and post-contrast T1 mapping was performed 10 minutes after contrast media injection (this approach was used for ECV measurements).

T1 mapping were obtained from three short-axis images (basal, center, apical) of the LV using Modified Look-Locker Imaging (MOLLI) technique. T2 mapping was carried out using a conventional T2-prepared single shot SSFP sequence. Table 1 presents the protocol parameters.

Table 1: Mapping protocols

Mapping	TR/TE (ms)	Slice thickness (mm)	Field of view (mm^2)	Acquisition matrix	No of slices
T1	3.44/1.58	8	320 × 360	342 × 384	5
T2	3.44/1.58	8	320 × 360	342 × 384	5

2.2 Data processing

MRI data in DICOM format were transferred to a workstation and processed using MATLAB (v. 2018; MathWorks, Natick, MA, USA).

2.2.1 Measurement of T1, T2 and ECV

Following image acquisition, T1 and T2 maps were generated from the MR workstation (uWS-MR, United Imaging Healthcare Co., Ltd., Shanghai, China). T1 times were measured from myocardium and blood pool region of interest (ROI) before and after contrast agent administration. Myocardial ROIs were used to measure T2 times. The estimation of ECV requires the assessment of myocardial and blood T1 values both before and after the administration of contrast agents, in addition to the patient's hematocrit level. The ECV formula is as follows:

$$ECV = (1 - hematocrit) \times (\Delta R1 myocardium / \Delta R1 blood),$$

where R1 = 1/T1

Figure 1 demonstrates the basal short-axis native T1, post-contrast T1, ECV, and T2 maps of a 25-year-old male without active cardiomyopathy. Figure 2 depicts the native T1, post-contrast T1 map, ECV map, and T2 map of a 55-year-old male diagnosed with dilated cardiomyopathy at the basal short-axis level. In comparison, figure 3 illustrates the same maps for a 79-year-old patient with ischemic cardiomyopathy. Standardized global and focal T1, T2 mapping, and ECV measurements were carried out in each of the case studies that were reported.

2.2.2 Diagnostic performance of the T1, T2 and ECV

Machine learning methods such as linear support-vector machine (SVM), Gaussian SVM, and linear discriminant analysis (LDA) were employed to evaluate the efficacy of T1, T2, and ECV in the clinical diagnosis of cardiomyopathies. The proposed framework presents a classification approach for differentiating between individuals without active cardiomyopathy (n=16) and those with active cardiomyopathy (n=16). Here, DCM and ICM were both considered the forms of active cardiomyopathy.

2.2.3 Statistical analysis

The diagnostic accuracy of the proposed classification was validated using 5-fold cross-validation. The sensitivity, specificity, accuracy, and area under the receiver-operating characteristic curve (AUC) were measured to evaluate the performance of classification. The paired *t*-test and boxplots were used to compare the T1, T2, and ECV values of the two groups.

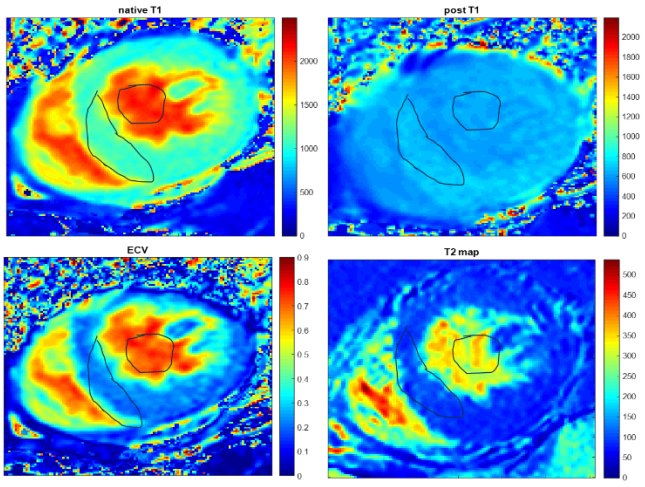

Figure 1: Representative images of native T1, postcontrast T1, extracellular volume fraction (ECV) map and T2 map of a 25-year-old without active cardiomyopathy subject. Region of interests for myocardium and blood pool regions are also shown. His left ventricle was normal (LV end-diastolic dimension=4.9 cm, volume=148 mL) and showed LV ejection fraction was 54

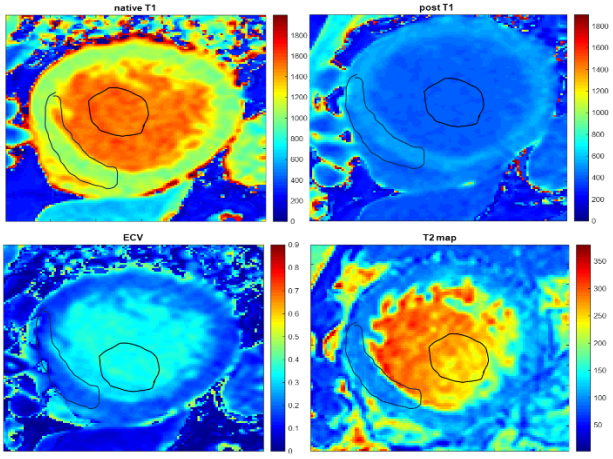

Figure 2: Representative images of native T1, postcontrast T1, extracellular volume fraction (ECV) map and T2 map of a 55-year-old with active dilated cardiomyopathy patient. Region of interests for myocardium and blood pool regions are also shown. His left ventricle was dilated (LV end-diastolic dimension = 7.06 cm, volume = 361 mL) and showed low LV ejection fraction (11.30%).

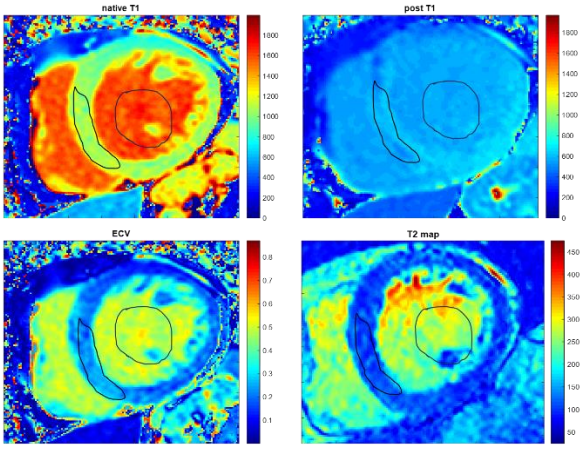

***Figure 3*:** Representative images of native T1, postcontrast T1, extracellular volume fraction (ECV) map and T2 map of a 79-year-old with chronic ischemic cardiomyopathy patient. Region of interests for myocardium and blood pool regions are also shown. His left ventricle end-diastolic dimension = 5.70 cm, volume = 360 mL) and showed low LV ejection fraction (24%).

3 Results

3.1 T1, T2 and ECV values

The mean native T1, T2 and ECV of myocardial regions in patients with active cardiomyopathy were 1315.45 ± 65 ms, 62.34 ± 7.26 ms and 32.72 ± 3.20% respectively, while patients without active cardiomyopathy had mean values of 1184.60 ± 67 ms, 53.12 ± 9.10 ms and 24.06 ± 3.52%. Patients Table 2 demonstrates the results of two class classification (without vs. with active cardiomyopathy) using three different maps and combinations of these maps. The combination of T1 and T2 achieved the sensitivity of 76.47 ± 1.23 %, specificity of 90.90 ± 1.59%, accuracy of 82.00 ± 2.05% and AUC of 0.78 using 5-fold cross-validation. The classification performance using ECV alone and for a combination of T1, T2 diagnosed with active cardiomyopathy had considerably ($p < 0.05$) greater native T1, T2 and substantially increased ECV values when compared to participants who did not have active cardiomyopathy. Boxplots comparing the T1, T2, and ECV values of the two groups are depicted in Figure 4.

3.2 Diagnostic performance using machine learning methods

and ECV was also evaluated. The linear SVM classifier achieved the highest performance with sensitivity of 92.30 ± 2.60 %, specificity of 86.67 ± 1.76 %, accuracy of 89.30 ± 1.95%, and AUC of 0.92 in two-class classification using a combination of T1, T2 and ECV. Figure 5 shows the ROC graphs for the two-class classifications using three different maps and combinations of these maps

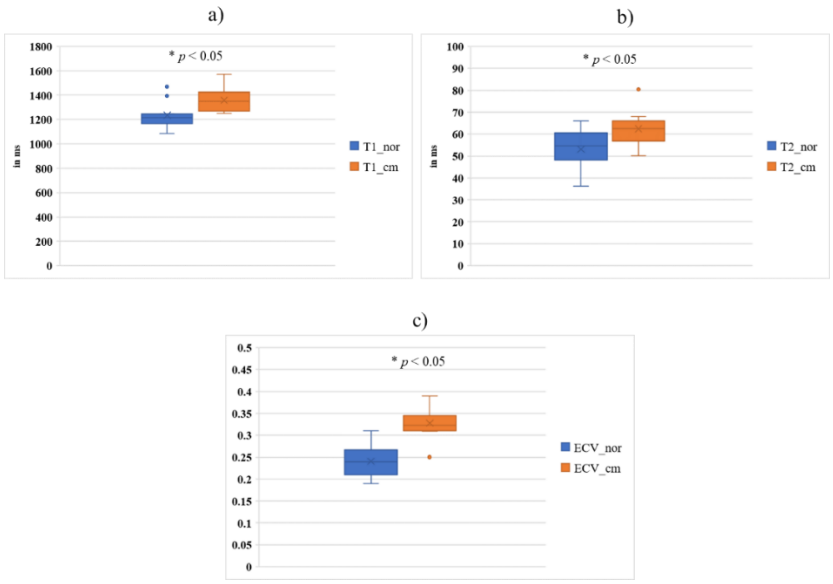

Figure 4: Boxplots for the comparison of T1, T2 and ECV blues between two groups. nor = Patients without active cardiomyopathy and cm = Patients without active cardiomyopathy.

Table 2: Classification performance of the proposed model for two class classification using 5-fold cross-validation.

Maps	Accuracy (%)	Sensitivity (%)	Specificity (%)	AUC
T1	75.00 ± 2.50	72.23 ± 1.45	80.00 ± 1.90	0.80
T2	67.90 ± 1.15	63.63 ± 1.50	58.50 ± 2.12	0.68
ECV	71.40 ± 1.20	72.00 ± 2.50	72.00 ± 1.90	0.84
T1+T2	82.00 ± 2.05	76.47 ± 1.23	90.90 ± 1.59	0.78
T1+T2+ECV	89.30 ± 1.95	92.30 ± 2.60	86.67 ± 1.76	0.92

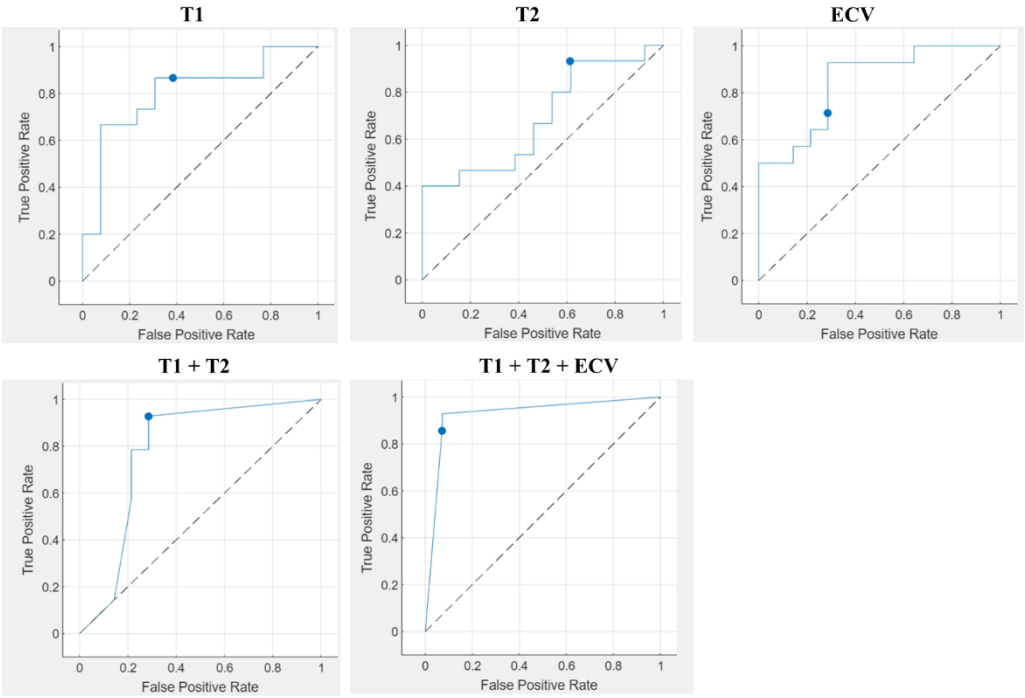

Figure 5: ROC graphs for the two-class classification using T1, T2 and ECV alone and the combination of these maps

4. Discussion

In this work, the role of T1 mapping, T2 mapping and ECV has been demonstrated in the diagnosis of cardiomyopathies (both dilated and acute ischemic cardiomyopathies) in a clinical setting.

These sequences are becoming increasingly available and are being utilized more frequently in clinical routine settings. Many studies in the recent literature demonstrated that mapping is an effective approach in the detection and measurement of global or diffuse cardiac processes without the necessity for endomyocardial biopsy [16]. According to Roller et al. (2015) [17], the application of mapping and ECV techniques exhibits significant promise in the assessment of prognostic indicators for various cardiac conditions. Furthermore, these measures can potentially serve as endpoints in clinical trials or aid in the monitoring of therapeutic interventions.

The T1, T2 mapping, and ECV have showed distinct advantages over alternative imaging techniques and sequences in the identification of early stages of several cardiomyopathies. This is primarily attributed to their ability to quantify T1 and T2 values at a voxel level, enabling the visualization of both local and global cardiac processes [17]. It has been found that native T1, T2 and ECV showed additional improvements in the diagnosis of cardiac diseases [18]. Nevertheless, it has still to be determined if the combination of mappings will play a significant role in the diagnosis of myocardial inflammation, offering enhanced diagnostic accuracy, rather than only being an additional feature in CMR settings.

The current study reported that patients diagnosed with active cardiomyopathy have higher levels of native T1 (1315.45 ± 65 ms vs. 1184.60 ± 67 ms), increased T2 (62.34 ± 7.26 vs. 53.12 ± 9.10 ms, $p < 0.05$), and significantly higher ECV expansion (32.72 ± 3.20% vs. 24.06 ± 3.52%) in comparison to patients who do not have active cardiomyopathy. The performance of the classification of active cardiomyopathy and no cardiomyopathy subjects was assessed by the T1, T2 mapping, and ECV individually, as well as in combination with T1, T2, and T1, T2, ECV. The classifier results showed that the incorporation of ECV together with T1 and T2 contributed to a significant improvement ($p<0.05$) in the classification accuracy (89.30% vs. 82%).

Furthermore, the combination of T1, T2 mapping and ECV may serve as a prognostic tool or provide additional diagnostic advantages. Additionally, it might contribute to a deeper

understanding of the underlying pathophysiology. However, there are some limitations of the study. One primary limitation of the study is the small sample size. The small sample size only offers initial indications regarding the diagnostic efficacy of mapping techniques; a large cohort and multicentre study can provide stronger evidence for larger clinical application. Furthermore, a direct comparison between native T1, T2, and ECV measurements and histological findings was not conducted due to the limited number of patients who had endomyocardial biopsy.

5. Conclusion

The integration of T1, T2, and ECV mapping techniques has showed encouraging outcomes in diagnosing of clinical cardiomyopathies, with an accuracy of 76% and AUC of 0.78. Furthermore, the implementation of these mapping techniques has the potential to consistently enhance the diagnosis of cardiomyopathies, which needs to be further evaluated with larger sample size.

6. Image/Figure Courtesy

All images are the courtesy of SSB Hospital, Faridabad, India.

7. References

1. Griffin BP, editor. Manual of Cardiovascular Medicine (4th Ed.). Philadelphia, PA: Lippincott Will José Marín-García,

2. Alimadadi A, Manandhar I, Aryal S, et al. Machine learning-based classification and diagnosis of clinical cardiomyopathies. Physiol Genomics. 2020;52: 391–400.

3. Yoon YE, Hong YJ, Kim HK, et al. 2014 Korean guidelines for appropriate utilization of cardiovascular magnetic resonance imaging: a joint report of the Korean Society of Cardiology and the Korean Society of Radiology. Korean J Radiol. 2014;15:659–688

4. Piechnik SK, Ferreira VM, Lewandowski AJ, et al. Normal variation of magnetic resonance T1 relaxation times in the human population at 1.5 T using ShMOLLI. J Cardiovasc Magn Reson. 2013;15:13

5. Burt JR, Zimmerman SL, Kamel IR, et al. Myocardial T1 mapping: techniques and potential applications. Radiographics 2014;34:377–395.

6. Kim PK, Hong YJ, Im DJ, et al. Myocardial T1 and T2 mapping: techniques and clinical applications. Korean J Radiol 2017;18:113–13

7. Piechnik SK, Ferreira VM, Dall'Armellina E, et al. Shortened Modified Look-Locker Inversion recovery (ShMOLLI) for clinical myocardial T1-mapping at 1.5 and 3 T within a 9 heartbeat breathhold. J Cardiovasc Magn Reson. 2010;12:69.

8. Dass S, Suttie JJ, Piechnik SK et al. Myocardial tissue characterization using magnetic resonance non contrast T1 mapping in hypertrophic and dilated cardiomyopathy. Circ Cardiovasc Imaging, 2012; 6: 726– 733

9. Ferreira VM, Piechnik SK, Dall'Armellina E et al. Non contrast T1 mapping detects acute myocardial edema with high diagnostic accuracy: a comparison to T2-weighted cardiovascular magnetic resonance. J Cardiovasc Magn Reason, 2012; 14: 42

10. Banypersad SM, Sado DM, Flett AS, et al. Quantification of myocardial extracellular volume fraction in systemic AL amyloidosis: an equilibrium contrast cardiovascular magnetic resonance study. Circ Cardiovasc Imaging 2013;6:34–39.

11. Thavendiranathan P, Walls M, Giri S et al. Improved detection of myocardial involvement in acute inflammatory cardiomyopathies using T2 Mapping. Circ Cardiovasc Imaging 2012; 5: 102–110

12. Kellman P, Hansen MS. T1-mapping in the heart: accuracy and precision. J Cardiovasc Magn Reson 2014;16:2.

13. Giri S, Shah S, Xue H, et al. Myocardial T2 mapping with respiratory navigator and automatic nonrigid motion correction. Magn Reson Med. 2012;68:1570–1578

14. Leiner T, Rueckert D, Suinesiaputra A, et al. Machine learning in cardiovascular magnetic resonance: basic concepts and applications. J Cardiovasc Magn Resonan. 2019; 21:61.

15. Martin-Isla C, Campello VM, Izquierdo C, et al. Image-Based Cardiac Diagnosis with Machine Learning: A Review. Front Cardiovasc Med. 2020;7:1.

16. P. Lurz, I. Eitel, J. Adam, et al. Diagnostic performance of CMR imaging compared with EMB in patients with suspected myocarditis. J Am Coll Cardiol Img, (2012); 5: 513-524

17. Roller FC, Harth S, Schneider C, et al. T1, T2 Mapping and Extracellular Volume Fraction (ECV): Application, Value and Further Perspectives in Myocardial Inflammation and Cardiomyopathies. Rofo. 2015;187(9):760-770.

18. Ntusi NA, Piechnik SK, Francis JM et al. Subclinical myocardial inflammation and diffuse fibrosis are common in systemic sclerosis--a clinical study using myocardial T1-mapping and extracellular volume quantification. J Cardiovasc Magn Reson. 2014;16:21..

Author Biography

Dr. Kamal Aggarwal

Director & Senior Consultant

Radiology Department,

SSB Hospital, Faridabad, Haryana, India

Dr. Kamal Aggarwal graduated with his MBBS from the University of Delhi in Delhi in 1993. He received his MD in 1998 in Radio Diagnosis/Radiology from the University of Delhi. He has 23 years of experience in the radiology field. Dr. Kamal Aggarwal practices at SSB Multispecialty Hospital in Sector 20A, Faridabad, India.

PASSION for CHANGE

If you have any questions about the magazine, or simply wish to reach out to us for any other reasons, you are welcome to contact us at the following email address: uinnovation-global@united-imaging.com